DEVELOPMENT OF VAPOUR COMPRESSION REFRIGERATION SYSTEM TEST RIG AND EVALUATION OF TEST DATA FOR R134A CONDENSATION IN COMPACT HEAT EXCHANGERS WITH SERRATED FIN

K V Ramana Murthy
Aeronautical Development Agency,
PB No.1718, Vimanapura Post
Bangalore, Karnataka, India
Email: katabathuni@gmail.com

C. Ranganayakulu
Aeronautical Development Agency, PB No.1718, Vimanapura Post
Bangalore, Karnataka, India
Email: r_chennu@hotmail.com

Mahesh Bondhu
Aeronautical Development Agency,
PB No.1718, Vimanapura Post
Bangalore, Karnataka, India
Email: maheshbondhuada@gmail.com

T P Ashok Babu
Mechanical Engineering Dept.,
National Institute of Technology Karnataka,
Surathkal, Karnataka, India
Email: tpashok@rediffmail.com

V.Vasudeva Rao
Mechanical & Industrial Engineering Dept.,
University of South Africa
Florida, South Africa
vasudvr@unisa.ac.za

ABSTRACT

Two phase flow analysis for the condensation of refrigerants within the compact plate fin heat exchangers is an area of ongoing research. Compact plate fin heat exchangers are becoming very popular due to their high effectiveness and compactness. This paper presents the sizing of compact plate fin heat exchanger and development of test rig to generate the Refrigerant (R134a) condensation heat transfer coefficient and pressure drop in Brazed Compact Plate Fin Heat Exchangers (BCPHE) with Serrated (Lance&Offset) fins. Also the theoretical design, manufacturing and testing of BCPHE for generation of R134a condensation heat transfer coefficient has been presented. CFD methodolgy has been used to develop the Single phase water side heat transfer coefficient and friction factor correlations for Serrated fin using ANSYS Fluent 14.5. The heat balance analysis has been carried out for calibration of the test rig using measured test data on both circuits and recorded a maximum deviation of 8%. Heat transfer coefficient for condensation of refrigerant R134a in compact heat exchangers with serrated fin is estimated using measured experimental data.

Key words: Vapour compression refrigeration test rig, Compact heat exchangers, heat transfer coefficient, Serrated fins, condenser, vacuum brazing, CFD analysis.

INTRODUCTION

In aircraft and automobile industry to meet the demand on performance, the volume and weight of the heat exchangers should kept minimum.Typically, a heat exchanger is called compact if the surface area density is greater than 700 m^2/m^3 in either one or more channels of a two stream or a multi-stream heat exchanger, as defined by Shah R.K et al.,[1].. There are also other actual and potential special applications in which compact heat exchanger passage geometry is needed to facilitate the highly efficient heating or cooling process involved in condensation or boiling.

Emperical correlations based on extensive experimental data have been obtained for the condensation heat transfer and frictional pressure drop characteristics of an ozone-friendly refrigerant HFC-134a (hydro fluorocarbon R134a) and other refrigerants in inside tubes and herringbone fins. Yi-Yie Yan et al.,[2] reported experimental data on condensation heat transfer and pressure drop of refrigerant R-134a in a vertical plate heat exchanger (PHE). The results indicated that the condensation heat transfer is slightly better for a higher average imposed heat flux, but the associated rise in frictional pressure drop (ΔP_f) was larger. H.J. Kang et al.,[3] and J.T. Han et al.,[4] studied on condensation of R-134a flowing inside helicoidal pipe. With the increase of mass flux, the overall condensation heat transfer coefficients of R134a increased, and slowly the pressure drops also increased. G.A.Longo et al.,[5] investigated the affect of enhanced surfaces on refrigerant condensation heat transfer coefficients. Jokar et al.,[6] studied condensation and evaporation of refrigerant R-134a in PHEs with a plate corrugation inclination angle of 60^o. Wang et al.,[7] obtained the pressure drop characteristics of complete and partial condensation in a PHE. They found that during steam condensation in the PHE, the condensate film flow was laminar initially but changed to turbulent flow very quickly in the wavy channel.

In phase change the heat transfer of a compact heat exchanger, in addition to fluid properties and geometrical parameters, the heat flux, mass flux and vapour quality also affect the heat transfer coefficients. Extensive experimental data and empirical correlations were obtained for the condensation heat transfer and pressure drop characteristics of refrigerant HFC-134a and other refrigerants on inside helicoidal pipe and Herringbone fins by Yi-Yie Yan et al.,[2]; HJ Kang et al.,[3]; G A Longo et al.,[5]; Giovanni A Longo,[8,9,10,11&12] and Amir Jokar et al.,[13]. However, none of these correlations can be used directly for the present study, where fin geometry is different, as these correlations do not have a predictive character.

The components holding the largest amount of refrigerant in a refrigeration unit are the condenser and evaporator.

Therefore Palm [14] indicated that, heat exchangers with small internal volume on refrigerant side should be used for same required system performance. Quantitative data are required before a heat exchanger can be designed and this data can be generated only through a dedicated experimental program accompanied by regorous or numerical analysis. The literature survey indicates that very limited research efforts have been devoted to the condensation of R134a in Compact plate heat exchangers ingeneral and only limited data is available for serrated type fin surfaces in particular in open literature.

NOMENCLATURE

A	Heat transfer area (m^2)
a	Ratio of fin area to total area
A_f	Free flow area (m^2)
C_p	Specific heat capacity (J kg^{-1} K^{-1})
DM	De-Mineralised
D_h	Hydraulic diameter (m)
FPI	Fins per inch
f	Fanning friction factor
G	Mass flux (kg m^{-2} s^{-1})
g	Acceleration due to gravity (m s^{-2})
H	Specific enthalpy (J kg^{-1})
h	Heat transfer coefficient (W m^{-2} K^{-1})
h	Fin height (m)
hp	Horse power
j	Colburn factor
l	Serration length (m)
m	Mass flow rate (kg s^{-1})
Nu	Nusselt number (hD_h / k), dimensionless
P	Pressure (bar)
Pr	Prandtl number (μC_p/k), dimensionless
P_s	Saturation pressure (bar)
Q	Heat load (kW)
q	Heat flux (kW m^{-2})
Re	Reynolds number
s	Fin spacing (m)
SCADA	Supervisory Controller & Data Acquisition System
T	Temperature (°C)
TR	Ton of refrigeration
T_s	Saturation temperature (°C)
T_w	Wall temperature (°C)
t	Fin thickness (m)
U	Overall heat transfer coefficient (W/m^2 K)
x	Vapor quality of refrigerant

Greek Symbols

ΔP	Pressure drop
ε	Turbulence dissipation rate,m^2/s^3
γ	Ratio of (t/s), dimensionless
k	Turbulent kinetic energy, m^2/s^2
λ	Thermal conductivity (W m^{-1} K^{-1})
μ	Dynamic viscosity, Ns/m^2
υ	Specific volume, m^3/kg
φ	Generalized transport variable
ρ	Density (kg m^{-3})
σ	Surface tension (N m^{-1})
Γ	Effective diffusivity, m^2/s^2
τ_w	Wall shear stress, N/m^2
η_f	Fin efficiency
η_o	Overall surface efficiency

Subscripts

a	air
i	inlet
l	liquid
o	overall
f	fin
w	wall
rsat	refrigerant saturation
eq	equivalent

EXPERIMENTAL SET-UP AND PROCEDURE:

The experimental test facility is established, to study the condensation of R134a in different types of serrated fins used in compact plate fin heat exchangers. Schematic diagram of the experimental test facility is shown in Figure 1, which has six main loops and SCADA system. Specifically, the system consists of a refrigerant loop, Condenser loop, Evaporator loop, cooling loop, super heater loop and de-super heater loop. Refrigerant R134a is circulated in the refrigerant loop, whereas De-mineralized (DM) water is used in all other loops. The condenser and evaporator loops are capable of supplying DM water flow at a constant temperature in the range of 5 ^{0}C to 60 ^{0}C. In order to obtain different conditions of R134a in the test heat exchanger, it is required to control the temperature and flow rate of the working fluids in the other loops.

Refrigerant Loop

The refrigerant loop contains the compressor rack, accumulators, oil separators, De-Super Heater, Condenser, test condenser (Brazed compact plate-fin heat exchanger), liquid receiver, filter drier, sight glasses, electronic expansion valve, evaporator, super heater and Coriolis flow meter. Refrigerant loop is a basic Vapour Compression Refrigeration System, consisting of four parallel semi hermitically sealed variable speed Reciprocating Compressors having different capacity, Test Condenser, Condenser, Electronic Expansion valve and Evaporator. Based on the total flow requirement and heat load capacity, four reciprocating compressors with variable frequency drive are selected. The variable speed reciprocating compressor rack is designed to control the flow rate between 0.01 kg/sec to 0.08 kg/sec in steps of 0.005 kg/sec using variable frequency drive. The flow rate was measured by a mass flow meter (Micro motion DN4) installed after the test condenser with an accuracy of ±0.05%. The details of compressor flow rates at different operating frequencies are listed in Table 1 and Table 2.

Table 1 Compressor Mass flow rate at different frequencies when the condenser temperature 20^{o}C and Evaporator temperature -10^{o}C.

S.No	Model No	Qty (No's)	Frequency(Hz)/ Flow rate(kg/sec)		
			30	35	50
1	2SB-34.07	1	0.0059	0.0069	0.009
2	2SB-38.2	1	0.008	0.009	0.0133
3	2SB-55.4	2	0.0213	0.0248	0.0354

In compressor suction line, accumulators are installed to prevent the liquid refrigerant return to suction line to an idled compressors. Oil separators are installed in the discharge line of each compressor. The oil separator intercepts the oil mixed with compressed gas and returns it to the crankcase of

the compressor thus assuring an efficient lubrication of its moving parts. The de-super heater installed in the downstream

Table 2 Compressor Mass flow rate at different frequencies when the condenser temperature 35.8°C and Evaporator temperature 20°C.

S.No	Model No	Qty (No's)	Frequency(Hz) / Flow rate(kg/sec)		
			30	35	50
1	2SB-34.07	1	0.0194	0.0227	0.03242
2	2SB-38.2	1	0.0249	0.0291	0.0415
3	2SB-55.4	2	0.0635	0.0741	0.105

of compressor rack, controls the inlet conditions of Test condenser by water cooling system. After condenser, the liquid refrigerant flows back to the receiver. The filter drier and collector tank are installed in the liquid line. The filter drier provides high water adsorption at low and high condensing temperatures, as well as at low and high degrees of humidity. The liquid line filter drier protects refrigeration system from moisture and solid particles. Coriolis flow meter is installed in the circuit after evaporator and after condenser to measure the refrigerant flow rate. The system also has sight glasses for physical verification of state of the refrigerant R134a. The standard Danfoss Brazed Plate heat exchanger (Type & Model: PHE B3-030-70-3.0-HQ Capacity: 27.5 kW) is installed in the main circuit for calibration of test rig. After attaining the required conditions the condenser is bypassed by the test heat exchanger which is installed as a separate test section. This test unit provides a water circuit to provide the cooling fluid, where the water flow rate can be varied between 0.08 kg/s to 0.7 kg/s. The pressure transducers and temperature sensors are located at the entrance and exit of the Test Condenser. The accuracy ranges of measuring devices are listed in the Table 3.

Table 3 Accuracy ranges of measuring devices

	Device	Type	Accuracy
1	Resistance thermometers	RTD	± 0.15°C
2	Thermocouples	Type K	± 0.5°C
3	Refrigerant flow meter	Coriolis effect	± 0.05%
4	Water flow meter	Turbine	± 0.25%
5	Pressure transducers	Stain gage type Range: 0-40bar g	± 0.25% full scale
6	Differential pressure transducers	Stain gage type Range:0-5 PSI	± 0.025% full scale

Brazed Compact Plate Fin Heat Exchanger:

Test Unit

The "Compact Heat Exchangers" by W.M. Kays and A.L. London [15], is used to carry out the theoretical thermal design of test units. Serrated fin surfaces with different fin heights, fin density are selected for two phase design data generation and analysis purpose. The schematic of the serrated fin geometry is shown in Figure 2. The flow in offset fins is highly turbulent even at low Reynolds number. The test unit is basically a cross flow arrangement with two passes on the water side and one pass on R134a side. The schematic representation of Test Core is shown in Figure 3. It is made of Aluminium alloy because of its low density, high thermal conductivity and high strength at low temperature. Considering the brazeability of aluminium alloy materials, Aluminium-Manganese alloy (AA3xxx) is selected for making fins. The geometric data of fins used in the test unit are given in Table 4.

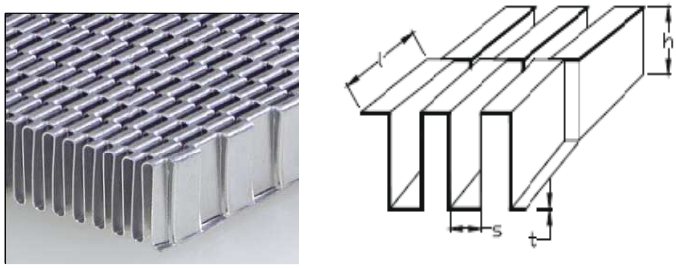

a) 3D view of Serrated Fin b) Serrated Fin dimensional notation

Figure 2 Schematics of Serrated fin geometry

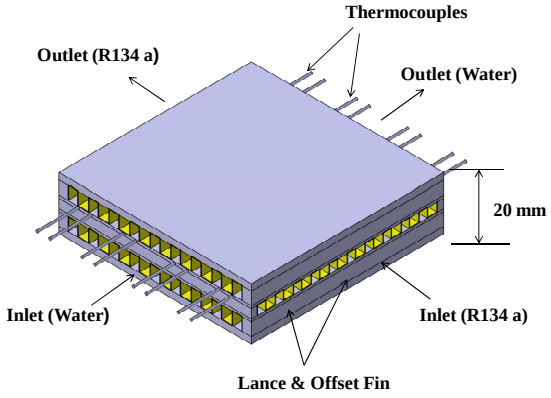

Figure 3 Schematic diagram of Test Unit Core

The basic principles of plate fin heat exchanger manufacture [16] are same for all sizes and materials. The fin surfaces, side-bars, parting sheets and cap sheets are held together in a jig under a predefined load, placed in a furnace and brazed to form the plate fin heat exchanger block. Vacuum brazing process is used for brazing of test units. The brazed Test Unit with inserted wires is shown in Figure 4. The stainless steel

(SS) wires are used to insert the thermocouples and these are removed after vacuum brazing. Thermocouples are inserted in the location from where SS wires are removed. The inserted thermocouples are fixed using conductive type adhesive. The headers and nozzles are then welded to the block, taking care that the brazed joints remain intact during the welding process.

Table 4 Geometric data of fins

Parameter	Unit	Value	
		DM Water side	Refrigerant side
Type		Lance & Offset	
Material		Aluminium AA-3003	
Fin frequency	FPI	28	
Fin height	mm	5	3
Fin thickness	mm	0.127	
Serration length	mm	3.175	3.175
No of layers		2	1
Total heat transfer area	m^2	0.7922	0.85506
Hydraulic diameter	mm	1.2271	1.3450

Figure 4 Brazed Test Unit

The brazed heat exchangers used in the experimental test facility to characterize the Serrated fins for the condensation of R134a, is shown in Figure 5. The exchanger including the inlet and outlet ports is 400 mm long. The cross sectional size of heat exchanger core is 150 mm x 150 mm. The heat exchanger considered here is of cross flow type with three surface fin layers.

The top and bottom layers are connected to water side and middle layer is connected to refrigerant side. To reduce the heat loss to the ambient, the entire test heat exchanger is wrapped with 10mm thick polyamide foam coated with hypalon. The average heat flux in the test heat exchanger was calculated by measuring the water temperature rise and water flow rate.

De-Super Heater

The de-super heater is placed between the compressor exit and Test condenser entry, in order to maintain the inlet refrigerant quality to the test unit. The standard Danfoss Brazed Plate heat exchanger (Capacity: 3 kW) is used as de-super heater. The vapour refrigerant flowing in the brazed plate heat exchanger was cooled to a required quality by the cold water flow. The de-super heater and the connection pipe between the test unit and the de-super heater were all thermally insulated with 10mm thick polyethylene.

Figure 5 Insulated Test Unit

Condenser Loop

The condenser loop in the system is designed for circulating the cold water through test unit. It contains 150 litre DM water bath with a 10kW heater and air cooler refrigeration unit of 6 TR cooling capacity intending to accurately control the water temperature. A water pump with 0.5 hp is used to drive the cold water to test unit with a specified water flow rate at constant inlet temperature.

Super Heater

The Super heater is placed between the evaporator exit and compressor entry, in order to ensure the entry of refrigerant to compressor in fully vapour form. Helical coil of $0.2m^2$ was used as super heater, which is dipped in 3kW capacity temperature bath. The refrigerant coming out from evaporator while passing through the helical tube was heated in the water bath before entering into the compressor. The super heater and the connection pipe between the evaporator and the super heater were all thermally insulated with 10mm thick polyethylene.

Data Acquisition

The data acquisition system is used, to collect the data of pressure, temperature, differential pressure, Water flow rate, refrigerant flow rate at different test points and the repeatability of experimental data is ensured. It includes the Industrial PC (IC200CPUE05) with 187 Channel Proficy HMI/SCADA-CIMPLICITY, which gives the measured data in the form of digital output. The pressure transducer, differential pressure transducer, turbine flow meter, Coriolis flow meter needs a power supply of 4-20 mA electric current as a driver for output.

Experimental Procedure

Initially the testing was carried out with industrial brazed PHE in condenser loop to calibrate the test facility. During operation, the vapour refrigerant R134a coming out from a compressor rack condenses in the condenser and the liquid refrigerant flows through Coriolis flow meter, collector tank and filter dryer. The quality of R134a at the condenser inlet was kept at desired value by adjusting the temperature and flow rate of DM water in De-Super heater. The liquid refrigerant then passes through evaporator after expansion in the electronic expansion valve. Any change of the system variables will lead to fluctuations in the temperature and pressure of the flow. The heat balance test is performed in the condenser and evaporator after the system reaching steady state and values are tabulated in Table 5. A deviation to the

extent of 10% was considered acceptable, and measured data was within the range. The photographs of experimental test facility along with control system and SCADA system are shown in Figure 6.

Table 5 Deviation of heat balance in condenser and Evaporator

S.No	Condenser			Evaporator		
	Qr (kW)	Qw (kW)	%Heat Balance	Qr (kW)	Qw (kW)	% Heat Balance
1	2.92	2.74	6.2	2.77	2.56	7.6
2	3.98	3.67	7.8	3.58	3.89	8.6
3	5.63	5.51	2.1	4.82	5.21	7.5

a) Test Facility

b) Test Unit Bench

c) Control & SCADA System

Figure 6 Photograph of Experimental Test Facility

The control valves are provided to facilitate connection between the condenser and Test Unit. Once the steady state condition is established, refrigerant is bypassed through Test unit by opening the solenoid valves through SCADA system. The readings of temperature, flow rate and pressure were logged using data acquisition system after stabilization of all the perameters. The stabilized test data is logged in SCADA system for a period of 10 sec. The average values of these measured data are used in the data reduction to obtain the refrigerant heat transfer coefficient. The thermal properties of the R134a were taken from thermophysical properties of refrigerants hand book [16].

DATA REDUCTION AND ANALYSIS

The data reduction and analysis is carried out in the present investigation to deduce the heat transfer rate from the refrigerant flow to the water flow in the test unit. The amount of heat transfer from the refrigerant to the water can be determined from the energy conservation principle. Therefore, the heat transfer from the refrigerant to the water can be calculated from the following equations:

$$Q_w = m_w C_{pw}(T_{wo} - T_{wi}) \quad (1)$$

Based on Newton's law of cooling, the overall heat transfer coefficient can be determined by

$$Q_w = UA_w\Delta T_{ln} \quad (2)$$

Where ΔT_{ln} , is the logarithm mean temperature difference defined as

$$\Delta T_{ln} = \frac{T_{wo} - T_{wi}}{\ln\frac{T_{rsat} - T_{wi}}{T_{rsat} - T_{wo}}} \quad (3)$$

Where T_{rsat} is the average saturation temperature of the refrigerant derived from the average pressure measured on refrigerant side and T_{wi} , T_{wo} are the water temperature at the inlet and outlet of the test unit. The average heat transfer coe it is derived fro ssuming no fou

a) Test Facility
b)Test Unit Bench
c) Control

$$\frac{1}{U} = \frac{}{\eta_{or}h_r} + \frac{}{\lambda\left(\frac{A_p}{A_r}\right)} + \frac{}{\eta_{ow}h_w\left(\frac{A_w}{A_r}\right)} \quad (4)$$

where A_w is the water side area, h_r and h_w are the refrigerant and water heat transfer coefficients respectively and η_0 is the overall fin surface efficiency, which is defined as;

$$\eta_o = 1 - a(1 - \eta_f) \quad (5)$$

in which 'a' is the ratio of the fin area to the total area,

$$\eta_f = \frac{\tanh(ml)}{ml} \quad (6)$$

Where $m = \sqrt{\frac{2h_w(1+\frac{t}{l})}{\lambda * t}}$ and $l = \frac{h}{2}$ (7)

Equation (4) shows that, if the heat transfer coefficient at the water side is known, the heat transfer coefficient h_r can be directly calculated from the experimental data. For general cases the Wilson plot technique could be used for finding both heat transfer coefficients as explained in Kumar R et.al.[18] and Styrylska TB et.al.,[19]. This method has been widely applied for separating individual resistances from an overall resistance. Unfortunately, due to lack of data, it is not possible to apply this method in the present investigation using the test

rig. Hence, the water side heat transfer coefficient h_w is estimated separately as explained in the following sections.

Water side heat transfer coefficient

Generally, the single-phase heat transfer coefficient can be expressed with the Colburn *j* factor,

$$j_w = \frac{h_w}{G\, c_p} Pr^{2/3} \qquad (8)$$

For the present fin geometry, the Reynolds number for water flow is defined as

$$Re_w = \frac{\rho V D_h}{\mu} = \frac{G D_{hw}}{\mu} \qquad (9)$$

Where

$$G = \frac{\dot{m}}{A_f} \qquad (10)$$

And

$$D_{hw} = [2(s-t)h]/[(s+h)+\frac{th}{l}] \qquad (11)$$

An extensive literature survey has been carried out to find a correct correlation on the water side heat transfer coefficient for lance and offset fin. The heat transfer coefficient and friction factor correlations presented by Pallavi P, Ranganayakulu C., [20], using CFD are compared with Weiting [21], Manglik RM and Bergles AE [22] and Joshi HM,Webb RL [23], which were obtained from the experiments with air flow. Sen Hu and Keith E Herold, [24-25] have published the affects of the Prandtl number on Colburn *j* factor for water and polyalphaolefin (PAO) fluids and claimed that, air models over-predict the *j* factor for liquids and found that the heat transfer coefficient of liquids is approximately 2 times larger than that of air. Hence, a detailed analysis has been carried out using ANSYS Fluent tool to estimate the '*j*' and '*f*' factors for Serrated fins in the following sections.

CFD analysis

The CFD analysis is carried out using ANSYS Fluent 14.5 for an estimation of *j* and *f* factors for offset fin geometry for water medium. In this model, a single layer of actual offset strip fin is modeled and meshed. The three-dimensional computational domain of fin model is shown in Figure 7. The offset strip fin is characterized for the laminar range of Reynolds number to determine the corresponding *j* and *f* values. In order to overcome the entrance effect, the concept of periodic fully developed flow as suggested by Patankar et.al.[26] is implemented for this part of analysis. The pressure drop obtained for unit length using ANSYS CFD fluent is used for estimation of the friction factor *f* as per, W.M. Kays and A.L. London [15] procedure. Similarly, the procedure is repeated for the range of Reynolds numbers from 100 to 800 in order draw the *f* versus Re curve. In this model, the "velocity inlet" and "outflow (pressure outlet)" boundary conditions are used at the inlet and outlet of the fin geometry, respectively. In the present analysis conjugate heat transfer effect is taken into account. The constant wall temperature boundary condition is employed for the walls as used by few authors earlier. The temperature difference between inlet and outlet of the core, in turn, is used for calculating the *j* factor using the Kays and London [15] methodology. The procedure is repeated for the turbulent range of Reynolds number to determine the corresponding *j* and *f* values.

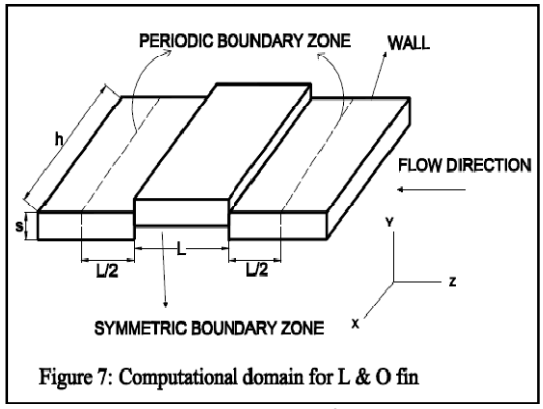

Figure 7: Computational domain for L & O fin

The velocity vector contours for the Reynolds numbers 10000 and 500 are shown in Figure 8 and Figure 9 for comparison of velocity magnitudes. From the velocity vectors it is quite clear that the flow is more laminar at Reynolds number 500 and is turbulent for the Reynolds number 10000.

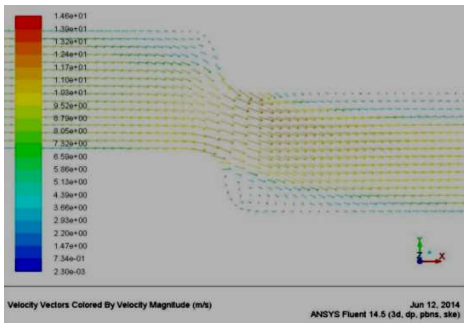

Figure 8 Velocity vector at Re=10000

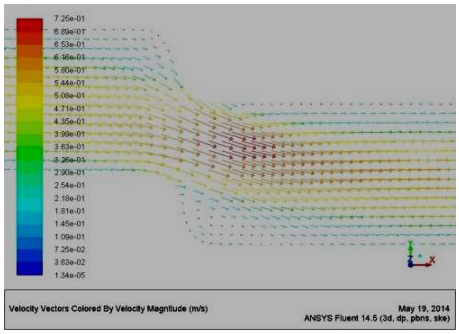

Figure 9 Velocity vector at Re=500

The pressure and temperature contours are shown in Fig.10 and Fig.11 respectively for the same fin surface.

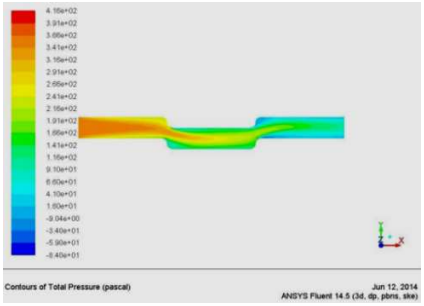

Figure 10 Pressure Contour at Re=500

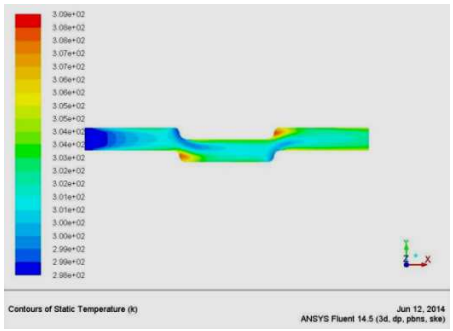

Figure 11 Temperature Contour at Re=10000

In addition, the results obtained from Fluent in the form of Colburn *j* and Fanning friction, *f* factors are compared with the correlationsavailable in the literature for air medium in Figure 12 and Figure 13 for laminar region and turbulent region respectively. According to Sen Hu and Keith E Herold, [24-25], there will be considerably a large deviation in *j* values of air with water due to a large difference in Prandtl number. It is observed that there is no significant deviation in *f* values when compared with air as observed by Sen Hu and Keith E Herold, [24-25]. Even though *j* is lower for water, the heat transfer coefficient, h_w is much higher when compared to air. The *f* vs. Re and *j* vs.Re data for serrated fin surface shows significant nonlinearity over the reynolds number range $100 \leq Re \leq 15000$. Therefore, two separate equations have been proposed for the low and the high Re regimes. The water side heat transfer coefficient h_w is calculated using a CFD analysis in accordance with Ranganayakulu et. al,[20,27,28]. The CFD estimated values are compared with experimental values presented by Wieting [21], Sen Hu and Keith E Herold, [24-25] and Byongjoo Kim, Byonghu Sohn[30]. Alternative dimensionless heat transfer coefficient often used for offset fin studies is the Colburn factor *j*, defined as

$$j_w = {Nu_w}\Big/{\left(Re * Pr^{\frac{1}{3}}\right)} \qquad (12)$$

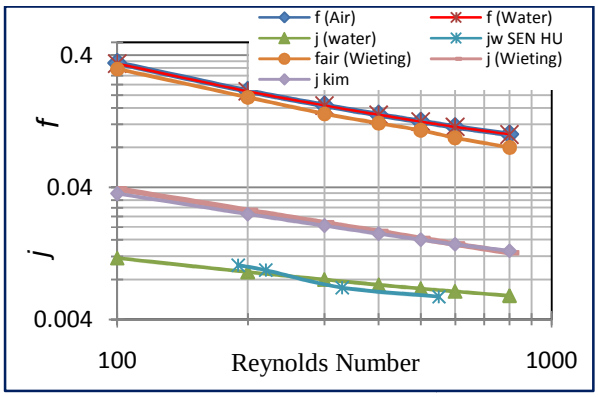

Figure 12 Colburn (*j*) & Friction factor (*f*) for Re : 100-800

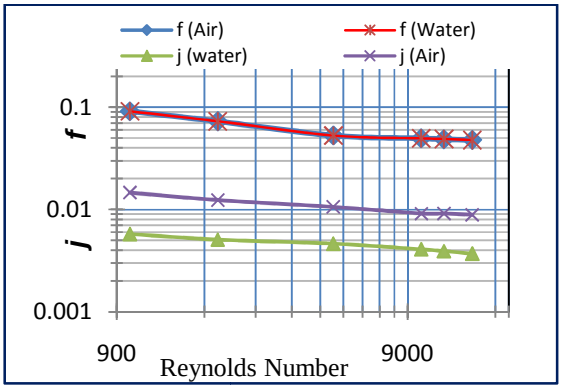

Figure 13 Colburn (*j*) and Friction factor (*f*) for Re : 1000-15000

Two phase condensation heat transfer

The procedures to calculate the condensation heat transfer coefficient of the refrigerant flow by using global overall heat transfer coefficient is given in Equation 4. Then, the refrigerant vapour quality entering the test unit is evaluated based on inlet conditions of pressure and temperature. Finally, the condensation heat transfer coefficient in the flow of R134a is calculated from the equation:

$$\frac{1}{h_r} = \eta_{or}\left(\frac{1}{U} - \frac{t}{\lambda\left(\frac{Ap}{Ar}\right)} - \frac{1}{\eta_{ow} h_w \left(\frac{A_w}{Ar}\right)}\right) \qquad (13)$$

Where h_w is determined from the empirical correlation for the single phase water to water heat transfer. Equivalent reynolds number [12] concept is used to partion the refrigerant flow region.

$$Re_{eq} = \frac{G\left[(1-x)+x\left(\rho_L/\rho_G\right)^{1/2}\right]D_h}{\mu_L} \qquad (14)$$

RESULTS AND DISCUSSION

Before running Condensation experiments with the test unit, the test rig main loop with industrial plate heat exchanger is operated by selecting a required compressors with suitable frequency and setting of the electronic expansion valve for the required pressure and flow rate conditions. The system was allowed to stabilize at the selected compressor speed, electronic expansion valve position and water side flow settings for at least 3 to 4 hours before taking inlet and outlet parameters of main loop condenser and evaporator. A set of readings were noted and observed to estimate the deviation in the heat balance in condenser side and found to be a maximum of 10%. As explained in CFD analysis section, the water side heat transfer coefficient h_w is estimated using a CFD analysis in accordance with Ranganayakulu et. al,[20,27]. The correlation for water side heat transfer coefficient and fanning friction factors for laminar range and turbulent range are as follows:

A. For Laminar Range ($100 \leq Re \leq 800$),

$$Nu_w = 0.049\, {Re_w}^{0.69} Pr^{\frac{1}{3}} \qquad (15)$$

Then, $$h_w = 0.049\, \left(\frac{\lambda_w}{D_h}\right) {Re_w}^{0.69} Pr^{\frac{1}{3}} \qquad (16)$$

$$f_w = 5.189 {Re_w}^{-0.596} \qquad (17)$$

B. For Turbulent Range ($1000 \leq Re \leq 15000$),

$$Nu_w = 0.016\, Re_w^{0.85} Pr^{\frac{1}{3}} \quad (18)$$

Then,

$$h_w = 0.016\, (\frac{\lambda_w}{D_h})\, Re_w^{0.85} Pr^{\frac{1}{3}} \quad (19)$$

$$f_w = 0.4533 Re_w^{-0.24} \quad (20)$$

Using the CFD correlations on water side, the heat transfer coefficient of refrigerant has been calculated for the serrated fin surface used in Test unit. Three different sets of saturated vapour condensation tests with refrigerant up-flow and water horizontal-flow are carried out at three different refrigerant saturation temperatures:25, 30 and 33.5^{0}C. Table 6 indicates the operating experimental test conditions in the test unit. Figure 14 and Figure 15 shows the effect of refrigerant mass flux and equivalent Reynolds number vs. refrigerant heat transfer coefficient for saturated vapour condensation at different saturation temperatures. Results indicate that the effect of saturation temperature is not much significant on heat transfer coefficient when the mass flux is less than 12 kg/m^{2}sec and probably condensation is controlled by gravity, which is shown in the Figure 14 and Figure 15. For higher refrigerant mass flux (>12 kg/m^{2}sec), the heat transfer coefficient depends on mass flux and forced convection condensation occurs. Figure.16 indicates the effect of mass flux vs. refrigerant heat flux, as the mass flux increases the refrigerant heat flux also increases. However, further experimentation is required to develop the two phase heat transfer coefficient correlations for different types of lance and offset fins. The results of the present experimental investigation adequately indicate that the experimental test rig/facility is working satisfactorily and two phase heat transfer coefficents are following the trends as discussed by earlier authors (Yi-Yie Yan et al.,[2]; HJ Kang et al.,[3]; G A Longo et al.,[5]; Giovanni A Longo,[8,9,10,11&12]).

Table 6 Operating Conditions during experimental tests

SI.No	P_{sat} (bar)	T_{sat} (^{o}C)	Quality		G_r	q_r
			x_{in}	x_{out}	(kg/m^{2}s)	(kW/m^2)
1	6.66	25	0.95-1	0-0.06	9.1-11.7	18.9-23
2	7.70	30	0.92-1	0-0.08	10.3-17.8	20.6-32
3	8.45	33.5	0.9-1	0-0.1	12.2-15.8	21.3-26.3

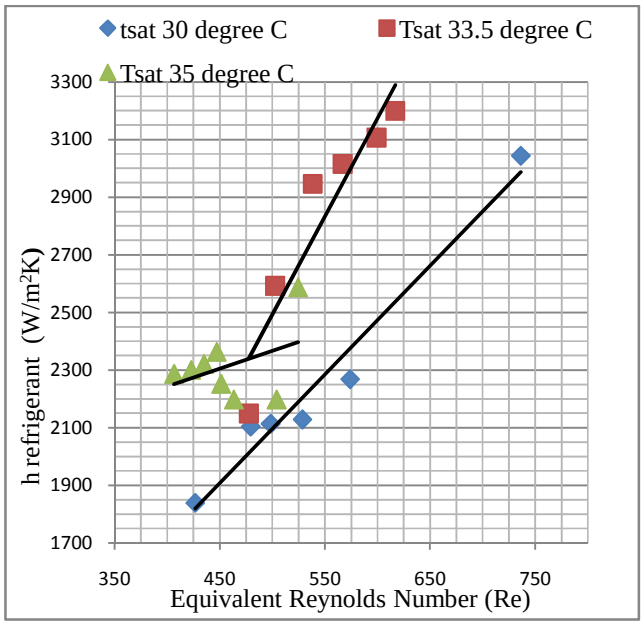

Figure 14 Refrigerant mass flux vs. Refrigerant heat transfer coefficient

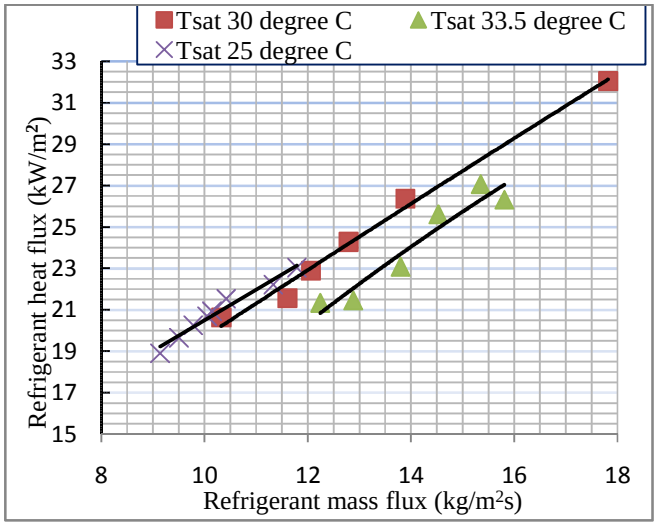

Figure 15 Equivalent Reynolds number vs. Refrigerant heat transfer coefficient

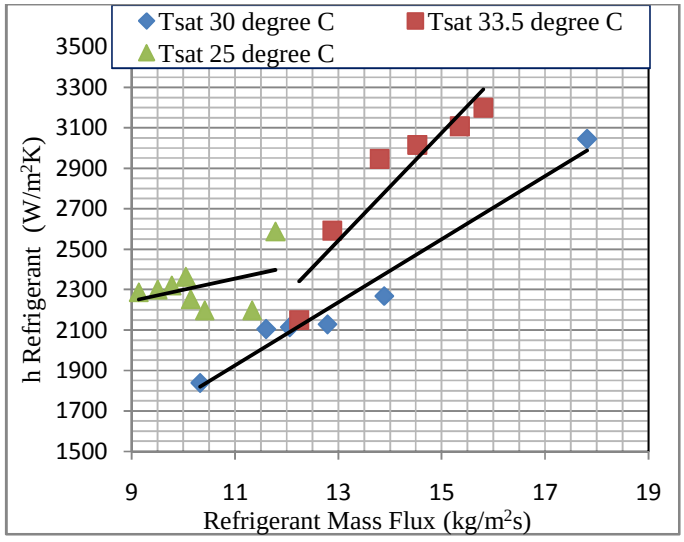

Figure 16 Refrigerant mass flux vs. Refrigerant heat flux

CONCLUSION

This paper presents the sizing of compact plate fin heat exchanger and development of test rig to generate the Refrigerant (R134a) condensation heat transfer coefficient and pressure drop in brazed compact plate fin heat exchangers (BCPHE) with Serrated (Lance&Offset) fins. Also the theoretical design, manufacturing and testing of BCPHE for generation of R134a condensation heat transfer coefficient has been discussed. CFD methodolgy has been developed for the Single phase water heat transfer coefficient and friction factor correlations for lance & offset fin using ANSYS Fluent 14.5. Heat balance analysis has been carried out for calibration of the test rig using measured test data on both circuits and recorded a maximum deviation of 8%. The effect of saturation temperature shall not be much significant on heat transfer coefficient when the mass flux is less than 12 kg/m^{2}s which corresponds to a liquid equivalent Reynolds number around 500 and probably condensation is controlled by gravity. For higher refrigerant mass flux (>12 kg/m^{2}s), the heat transfer coefficient depends on mass flux and forced convection condensation occurs.

Acknowledgement

The Authors wish to acknowledge Aeronautical Development Agency for allowing publication of the paper.

References

[1] **Shah R.K., S. Kakac , A.E.Bergles, F.Mayinger**, Heat exchangers – *Thermal hydraulic fundamentals and design, Hemisphere Publishing Corp., Washington DC*, 9-46(1980).

[2] **Yi-Yie Yan, Hsiang-Chao Lio, Tsing-Fa Lin**, Condensation Heat transfer and Pressure drop of refrigerant R-134a in a plate heat exchanger, *Int. J. Heat and Mass Transfer* 42 (1999) 993-1006.

[3] **H.J. Kang, C.X. Lin, M.A. Ebadian**, Condensation of R134a flowing inside helicoidal pipe, *Int. J. Heat and Mass Transfer* 43 (2000) 2553-2564.

[4] **J.T. Han a,T, C.X. Lin b, M.A. Ebadian**, Condensation heat transfer and pressure drop characteristics of R-134a in an annular helical pipe, *International Communications in Heat and Mass Transfer* 32 (2005) 1307-1316.

[5] **G.A. Longo, A. Gasparella, R. Sartori**, Experimental heat transfer coefficients during refrigerant vaporisation and condensation inside herringbone-type plate heat exchangers with enhanced surfaces, *International Journal of Heat and Mass Transfer* 47 (2004) 4125-4136.

[6] **A. Jokar, S.J. Eckels, M.H. Hosni, T.P. Gielda**, Condensation heat transfer and pressure drop of the brazed plate heat exchangers using R-134a, *Journal of Enhanced Heat Transfer* 11 (2) (2004) 161–182.

[7] **L.K. Wang, B. Sunde´n, Q.S. Yang**, Pressure drop analysis of steam condensation in a plate heat exchanger, *Heat Transfer Engineering* 20(1)(1999)71–77.

[8] **Longo, G.A.**,Gasparella, A., Refrigerant R134a vaporisation heat transfer and pressure drop inside a small brazed plate heat exchanger, *International Journal of Refrigeration* 30 (2007) 821-830.

[9] **Giovanni .A. Longo**, Refrigerant R134a condensation heat transfer and pressure drop inside a small brazed plate heat exchanger, *International Journal of Refrigeration* 31 (2008) 780-789.

[10] **Giovanni .A. Longo**, R410A condensation inside a commercial brazed plate heat exchanger, *Experimental Thermal and Fluid science* 33 (2009) 284-291.

[11] **Giovanni A.Longo**, Heat Transfer and pressure drop during hydrocarbon refrigerant condensation inside a brazed plate heat exchanger, *International Journal of Refrigeration* 33 (2010) 944-953.

[12] **Giovanni A.Longo, Claudio Zilio**, Condensation of the low GWP refrigerant HFC1234yf inside a brazed plate heat exchanger, *International Journal of Refrigeration* 36 (2013) 612-621.

[13] **Amir Jokar , Mohammad H. Hosni , Steven J. Eckel**, Dimensional analysis on the evaporation and condensation of refrigerant R-134a in minichannel plate heat exchangers, *Applied Thermal Engineering* 26 (2006) 2287–2300.

[14] **Palm B.,**Refrigeration systems with minimum charge of refrigerant. *Applied Thermal Engineering* 27 (2007) 1693-1701.

[15] **W.M. Kays, and A.L. London**, Compact Heat Exchangers, 3rd Edition, McGraw-Hill, New York, 1984.

[16] **ALPEMA**, The standards to the Brazed Aluminium Plate Fin Heat Exchanger Manufactures Association (http://www.alpema.org/).

[17] **ASHRAE** Fundamental hand book, , *Thermophysical propertiesof refrigerants* (2001).

[18] **Kumar R, Varma HK, Agrawal KN, Mohanty B**, A comprehensive study of modified Wilson plot technique to determine the heat transfer coefficient during condensation of steam and R-134a over single horizontal plain and finned tubes. *Heat Transfer Engineering* 22(2001):3-12.

[19] **Styrylska TB, Lechowska AA,** Unified Wilson Plot Method for Determining Heat Transfer Correlations for Heat Exchangers. *Transactions of ASME*(2003), 125:752.

[20] **Pallavi P, Ranganayakulu C,** Development of Heat transfer coefficient and friction factor correlations for offset fins using CFD, *Int. Journal of Numerical Methods for heat and fluid flow* (2011), Volume 21, No.8.

[21] **Wieting AR,** Empirical correlations for heat transfer and flow friction characteristics of rectangular offset-fin plate-fin heat exchangers. *J Heat Transfer*(1975), 97:488-490.

[22] **Manglik RM, Bergles AE**, Heat transfer and pressure drop correlations for the rectangular offset fin compact heat exchanger. *J Experimental Thermal and Fluid Science*(1995), 10:171-180.

[23] **Joshi HM, Webb RL**, Heat transfer and friction in the offset strip-fin heat exchangers. *Int J Heat Mass Transfer* (1987), 30:69-84.

[24] **Sen Hu S, Keith E Herold**, Prandtl number effect on offset fin heat exchanger performance: predictive model for heat transfer and pressure drop. *Int J Heat Mass Transfer* (1995), 38:1043-1051.

[25] **Sen Hu S, Keith E Herold**, Prandtl number effect on offset fin heat exchanger performance: experimental results. *Int J Heat Mass Transfer*(1995), 38:1053-1061.

[26] **Patankar, S.V., Liu, C.H. and Sparrow, E.** Fully Developed Flow and Heat Transfer in Ducts Having Streamwise-Periodic Variations of Cross-Sectional Area, *Journal of Heat Transfer*(1977), Vol.99, pp.180-186.

[27] **Ranganayakulu C, Iris Mersmann, Stephan Kabelac**, Boiling of R134a in a plate fin heat exchanger having offset fins. In proceedings of the 11th International ISHMT-ASME *Heat and Mass Transfer onference*, HMTC11300040, (2013) Dec 28-31, IIT Kharagpur, India.

[28] **Ismail LS, Ranganayakulu C, Shah RK**, Numerical study of flow patterns of compact plate-fin heat exchangers and generation of design data for offset and wavy fins. *In: Proceedings of 6th International conference on Enhanced, Compact and Ultra-compact Heat Exchangers: Science, Engineering and Technology*, CHE2007-0016, Potsdam, Germany, (2007)Sept 16-21, pp. 113-122.

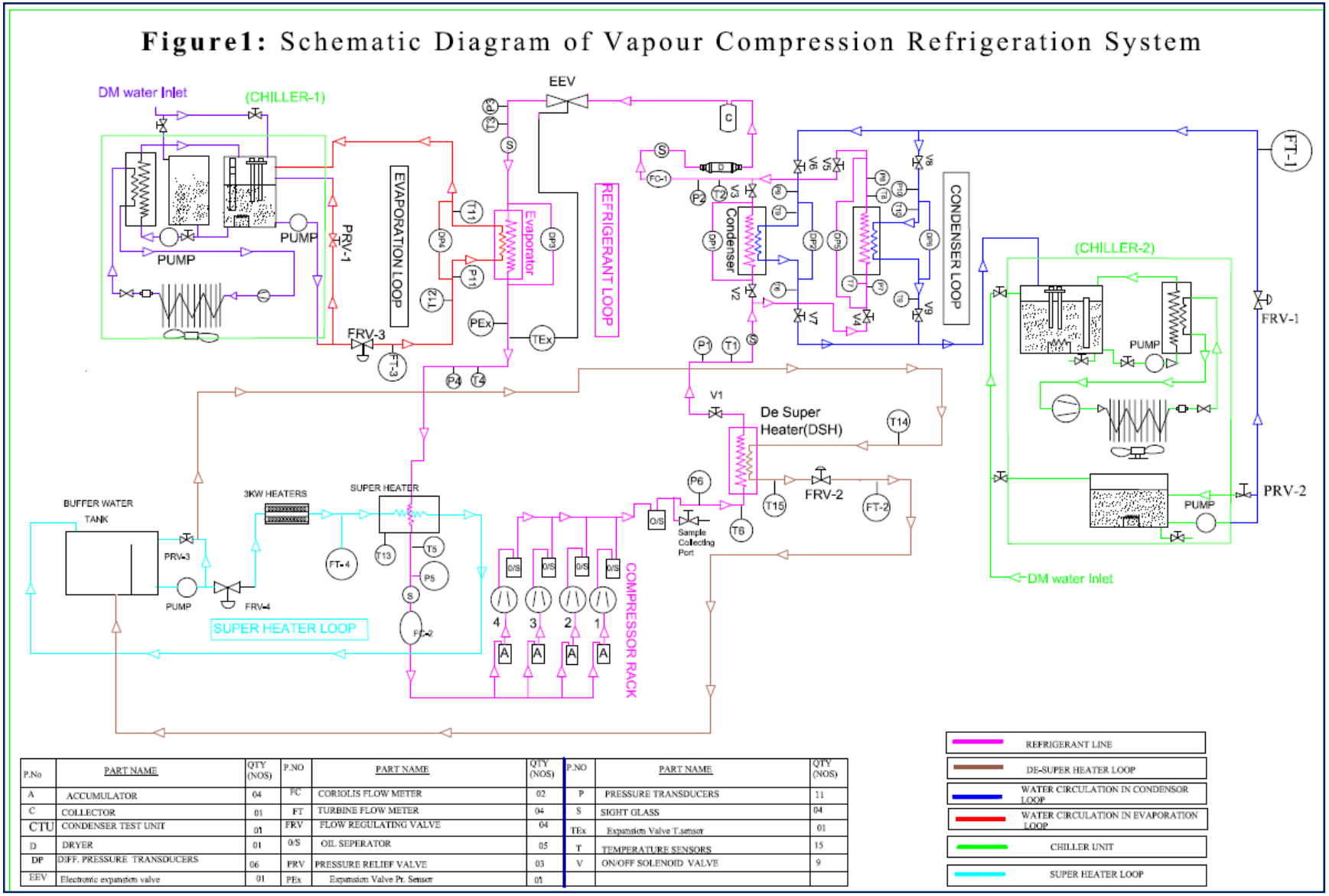

P.No	PART NAME	QTY (NOS)	P.NO	PART NAME	QTY (NOS)	P.NO	PART NAME	QTY (NOS)
A	ACCUMULATOR	04	FC	CORIOLIS FLOW METER	02	P	PRESSURE TRANSDUCERS	11
C	COLLECTOR	01	FT	TURBINE FLOW METER	04	S	SIGHT GLASS	04
CTU	CONDENSER TEST UNIT	01	FRV	FLOW REGULATING VALVE	04	TEx	Expansion Valve T.sensor	01
D	DRYER	01	O/S	OIL SEPERATOR	05	T	TEMPERATURE SENSORS	15
DP	DIFF. PRESSURE TRANSDUCERS	06	PRV	PRESSURE RELIEF VALVE	03	V	ON/OFF SOLENOID VALVE	9
EEV	Electronic expansion valve	01	PEx	Expansion Valve Pr. Sensor	01			

Figure 1 Schematic Diagram of Vapour Compression Refrigeration System